



0040-4020(94)00556-7

NEW SUPRAMOLECULAR HOST SYSTEMS. 1. A STRUCTURAL AND CONFORMATIONAL STUDY OF THE 1,3,5,7-TETRAOXADECALIN CORE SYSTEM¹Hanoch Senderowitz^a, Anthony Linden^b, Larisa Golender^a, Sarah Abramson^a and Benzion Fuchs^{a*}^a) School of Chemistry**, Tel-Aviv University, Ramat-Aviv, 69 978 Tel-Aviv, Israel^b) Organisch-chemisches Institut, Universität Zürich, Winterthurerstrasse 190, CH-8057 Zürich, Switzerland

Abstract: This is the first in a series of studies of new host systems based on the 1,3,5,7-tetraoxadecalin (TOD) core moiety. The parent molecule (2) and its 2,6-di(trans-styryl) derivative (5) were studied in the crystal (low temperature X-ray diffraction, electron density, geometry) and in solution (static and dynamic NMR). The relative energies from the solution studies and the structural parameters from the X-ray analysis were compared with those from a ring-fragment analysis and with structural data of 1,3-dioxanes and 1,3,5,7-tetraoxadecalins which were retrieved from the Cambridge Structural Database. Molecular mechanics calculations using MM2 and MM3 performed poorly in reproducing relative energies and structural parameters. This is attributed to stereoelectronics in the 1,3,5,7-TOD system.

INTRODUCTION

We have recently initiated a new research project on novel polyacetal macromolecules, viz., polymers or macrocycles bearing "core" molecules based on 1,3,5,7-tetraoxadecalin (1,3,5,7-TOD). The 1,3,5,7-TOD system exists in the *trans* (1) and *cis* configurations, with the latter occurring in two conformationally interconverting forms, "O-inside" (2) and "O-outside" (3) (Figure 1). Contrary to the well known *cis*-decalin system² or its 1,4,5,8-tetraoxa derivative³, which exist as racemic mixtures of fast interconverting enantiomers 4 \rightleftharpoons 4', the relationship between 2 and 3 is diastereomeric.

The 1,3,5,7-TOD system is long known in carbohydrate chemistry⁴. The preparation of the parent, unsubstituted molecules has been described⁵⁻⁷ and the *cis*-O-inside (2) form was discussed by Howard and Lemieux⁵, while the relative stabilities of certain substituted *cis*-1,3,5,7-TOD derivatives were examined by Stoddart⁷, Schroll⁶ and coworkers. The starting materials in the preparative procedure actually determine the configuration of the 1,3,5,7-TOD products. Thus, (Figure 1) acetalization of erythritol with formaldehyde yields *trans*-1,3,5,7-TOD (1) while D-threitol gives *cis*-1,3,5,7-TOD (2, 3) (these are accompanied by other, minor acetalic byproducts, e.g., 4,4'-bi(dioxolyl) which, since they are not discussed in this study, are not shown in Figure 1). Indeed, the *meso* character of erythritol is preserved in the centrosymmetric 1 (C₁) molecule, while C₂ of threitol is preserved in 2 and 3.

While we are interested in the entire 1,3,5,7-TOD system, the immediate subject of our research was the *cis*-O-inside isomer (2) which bears four oxygen atoms directed into its built-in cavity. We anticipated that the latter will be able to provide a good *host* environment in suitably substituted

* Author for correspondence. Dedicated to Professor Alan R. Katritzky

** Part of the Raymond and Beverly Sackler Faculty of Exact Sciences at Tel-Aviv University.

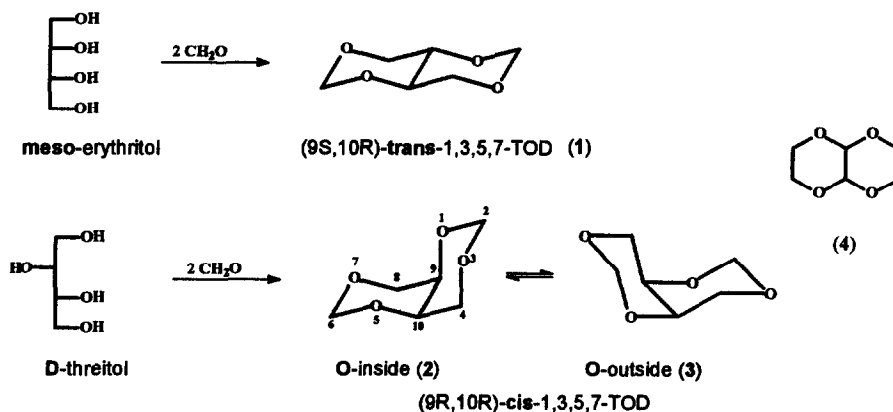
systems, which are currently being built and studied in our group^{9,10}.

In this paper we elaborate on the structural features of **2** and **5** in the solid state and compare these results with those available by retrieval from the Cambridge Structural Database (CSD) of some literature TOD structures and of the constituting ring fragments. The electronic properties are inferred and the dynamic behaviour in solution of **2** and **3** is described. We felt also compelled to probe in detail, using contemporary tools of experimental and computational interrogation, the static and dynamic behavior of the *cis*-1,3,5,7-tetraoxadecalin core system, but we found that the MM2 and MM3 force fields are inadequate in calculating these features.

RESULTS AND DISCUSSION

To gain a good understanding of *cis*-1,3,5,7-TOD, in particular to probe possible electron density manifestations of high lone-pair concentrations in small elements of space and to obtain accurate geometries, we set out to determine the low-temperature crystal structures of two molecules in this system. Some room-temperature X-ray diffraction analyses of substituted 1,3,5,7-TOD compounds in the series have been published¹¹. For that of the "naked" *trans* isomer (**1**), partial structural data have been quoted¹², but we could not find the full report. As to the unsubstituted *cis*-O-outside form (**3**),

Figure 1. The three 1,3,5,7-tetraoxadecalin (1,3,5,7-TOD)[†] diastereomers and their derivation from the respective tetritols.



[†] For the sake of clarity and consistency with all our and certain other studies, we use the 1,3,5,7-tetraoxadecalin nomenclature (*cf.* **2** for atom numbering). Other names are, *e.g.* for *cis*-1,3,5,7-TOD: (1*R*)-*cis*-2,4,7,9-tetraoxabicyclo[4.4.0]decane, 1,3:2,4-di-O-methylene-*D*-threitol or (as in Chemical Abstracts), (4*aR*)-(4*aR*,8*ac*)-tetrahydro[1,3]dioxino[5,4-*d*]-1,3-dioxin. In the same context, due to a minor but basic omission of the CIP rules, one cannot assign configurations to chiral *cis*-decalin (and similar) systems, other than by 9,10-helicity specification. Thus, the diastereoisomers **2** ("O-inside") and **3** ("O-outside") are, in fact, (9*R*; 9,10-*M*)- and (9*R*; 9,10-*P*)-*cis*-1,3,5,7-tetraoxadecalin, respectively.

although observed in solution, it is practically unisolable. Hence, we prepared single crystals of *rac-cis*-1,3,5,7-tetraoxadecalin (2) and of (9*R*;9,10-*M*)-2,6-di(*trans*-styryl)*cis*-1,3,5,7-tetraoxadecalin (5)^{10a}, which were submitted to low temperature X-ray diffraction analysis. Thus, we were able to secure accurate molecular structural parameters and to probe the electron density in the peculiar molecular cavity, into which the oxygen electron lone-pairs are projected.

Table 1. Experimental details of X-ray diffraction analyses of *cis*-1,3,5,7-tetraoxadecalin (2) and its 2,6-di(*trans*-styryl) derivative (5).

A. Crystal Data	(2)	(5)
Empirical Formula	C ₆ H ₁₀ O ₄	C ₂₂ H ₂₂ O ₄
Formula Weight	146.14	350.41
Crystal Color, Habit	colourless, prism	colourless, plate
Crystal Dimensions (mm)	0.17 x 0.28 x 0.38	0.10 x 0.50 x 0.50
Crystal System	monoclinic	monoclinic
No. of Reflections Used for Unit Cell Determination (2θ range)	25 (30-34°)	18 (24-26°)
Lattice Parameters:	a = 14.006 (3) Å b = 4.4705 (9) Å c = 13.314 (2) Å β = 131.02 (1)° V = 629.0 (2) Å ³	a = 7.541 (2) Å b = 8.497 (2) Å c = 14.522 (2) Å β = 99.35 (3)° V = 918.2 (3) Å ³
Space Group	C2/c (#15)	P2 ₁ (#4)
Z value	4	2
D _{calc}	1.543 g cm ⁻³	1.267 g cm ⁻³
F(000)	312	372
μ (MoK _α)	1.222 cm ⁻¹	0.810 cm ⁻¹
B. Intensity Measurements		
Diffractometer	Nicolet R3	Rigaku AFC5R
Radiation	MoK _α (λ = 0.71069 Å)	MoK _α (λ = 0.71069 Å)
Temperature	123 K	100 K
Scan Type	ω-2θ	ω-2θ
Scan Rate	2.9 - 29.3° min ⁻¹	8° min ⁻¹
Scan Width	2.2+(2θ _{Kα₁} - 2θ _{Kα₂})	1.37+0.35 tanθ
2θ(max)	70°	109°
No. of Reflections Measured	Total: 4773 Unique: 1402 (R _{int} = 0.024)	Total: 24048 Unique: 12052 (R _{int} = 0.040)
Corrections	Lorentz-polarization.	No decay. No extinction correction
Absorption (max. & min. coeff.):	1.051 - 0.872	1.135 - 0.741
C. Structure Solution and Refinement		
Structure Solution	Direct methods ²¹	
Refinement	Full-matrix least-squares on F ²²	
Function Minimized	Σw(F _o - F _c) ²	
Least-square Weights	[σ ² (F _o) + (0.015F _o) ²] ⁻¹	[σ ² (F _o) + (0.005F _o) ²] ⁻¹
No. Observations (I > 3σ(I))	983	6055
No. Variables	66	322
Reflection/Parameter Ratio	14.9	18.8
Residuals: R; R _w	0.0270; 0.0375	0.0343; 0.0332
Goodness of Fit Indicator	1.635	1.693
Max. Shift/Error in Final Cycle	0.0001	0.001
Max. & Min. Peak in Final Difference Map	0.27; -0.34 e Å ⁻³	0.28; -0.26 e Å ⁻³

The experimental details are presented in Table 1, the structural data in Tables 2 and 3 and the ORTEP diagrams in Figures 2 and 3. The structure of **2** contains a crystallographic 2-fold axis passing through the mid point of the C9-C10 bond (crystallographically designated C9-C9'). Molecular packing diagrams, showing the racemic **2** and enantiopure **5**, are presented in Figures 4 and 5, respectively.

Figure 2. An ORTEP drawing of *cis*-1,3,5,7-tetraoxadecalin (**2**) with 50% probability ellipsoids showing the atom numbering (atoms O5, O7, C6, C8 & C10 are equivalent to O1, O3, C2, C4 & C9, respectively).

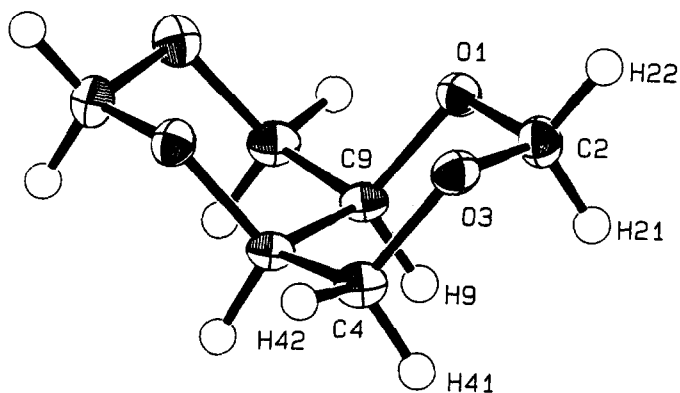


Figure 3. An ORTEP drawing of (9*R*)-2,6-di-*p*-(*trans*-styryl)-*cis*-1,3,5,7-tetraoxadecalin (**5**) with 50% probability ellipsoids, showing the atom numbering.

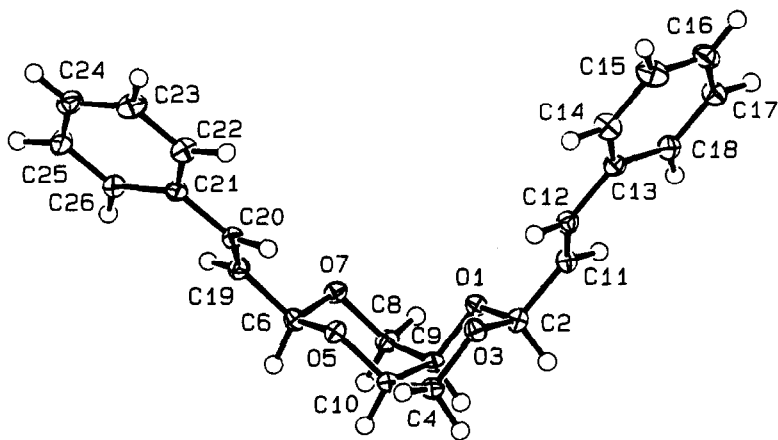


Table 2. Atomic positional parameters and equivalent isotropic temperature factors (\AA^2) of *cis*-1,3,5,7-tetraoxadecalin (2) with e.s.d.s in parentheses. A crystallographic C2 axis through C(9)-C(10) makes atoms O5, O7, C6, C8 & C10 equivalent to O1, O3, C2, C4 & C9, respectively.

ATOM	x	y	z	Ueq*
O(1)	0.12881(5)	0.0156(1)	0.38179(5)	0.0194(3)
O(3)	0.12375(5)	-0.0115(1)	0.20260(6)	0.0220(3)
C(2)	0.20038(7)	0.0220(2)	0.34174(8)	0.0223(4)
C(4)	0.03736(7)	0.2348(2)	0.13554(8)	0.0208(4)
C(9)	0.04233(7)	0.2632(2)	0.32578(7)	0.0173(3)

*Ueq is defined as one third of the trace of the orthogonalized Uij tensor

Table 3. Atomic positional parameters and equivalent isotropic temperature factors (\AA^2) of 2,6-di-*p*-(*trans*-styryl)-*cis*-1,3,5,7-tetraoxadecalin (5) with e.s.d.s in parentheses.

ATOM	x	y	z	Ueq*
O(1)	0.34006(8)	0.5282(1)	0.90142(4)	0.0164(1)
C(2)	0.1630(1)	0.5102(1)	0.85277(6)	0.0174(2)
O(3)	0.04242(9)	0.4670(1)	0.91411(4)	0.0182(2)
C(4)	0.0329(1)	0.5885(1)	0.98175(6)	0.0191(2)
O(5)	0.27379(8)	0.5	1.09758(4)	0.0168(1)
C(6)	0.4509(1)	0.5233(1)	1.14612(5)	0.0169(2)
O(7)	0.57686(8)	0.5275(1)	1.08372(4)	0.0174(1)
C(8)	0.5416(1)	0.6596(1)	1.02105(6)	0.0186(2)
C(9)	0.3514(1)	0.6545(1)	0.96810(6)	0.0167(2)
C(10)	0.2177(1)	0.6283(1)	1.03514(6)	0.0168(2)
C(11)	0.1671(1)	0.3860(1)	0.77989(6)	0.0189(2)
C(12)	0.0756(1)	0.2519(1)	0.77584(6)	0.0184(2)
C(13)	0.0708(1)	0.1285(1)	0.70423(6)	0.0170(2)
C(14)	-0.0262(1)	-0.0098(2)	0.71223(7)	0.0244(2)
C(15)	-0.0369(2)	-0.1275(2)	0.64438(8)	0.0294(3)
C(16)	0.0495(1)	-0.1085(2)	0.56759(7)	0.0259(3)
C(17)	0.1464(1)	0.0283(2)	0.55878(6)	0.0241(2)
C(18)	0.1576(1)	0.1453(1)	0.62637(6)	0.0211(2)
C(19)	0.5006(1)	0.3917(1)	1.21409(6)	0.0181(2)
C(20)	0.3966(1)	0.2670(1)	1.22193(6)	0.0169(2)
C(21)	0.4347(1)	0.1383(1)	1.29025(5)	0.0166(2)
C(22)	0.3339(1)	-0.0007(1)	1.27774(7)	0.0219(2)
C(23)	0.3643(2)	-0.1229(2)	1.34249(8)	0.0268(3)
C(24)	0.4949(1)	-0.1070(2)	1.42160(7)	0.0251(3)
C(25)	0.5959(1)	0.0303(2)	1.43495(6)	0.0240(2)
C(26)	0.5662(1)	0.1520(1)	1.37018(6)	0.0204(2)

*Ueq is defined as one third of the trace of the orthogonalized Uij tensor

Figure 4. Molecular packing of *rac*-*cis*-1,3,5,7-tetraoxadecalin (2) projected down the c-axis.

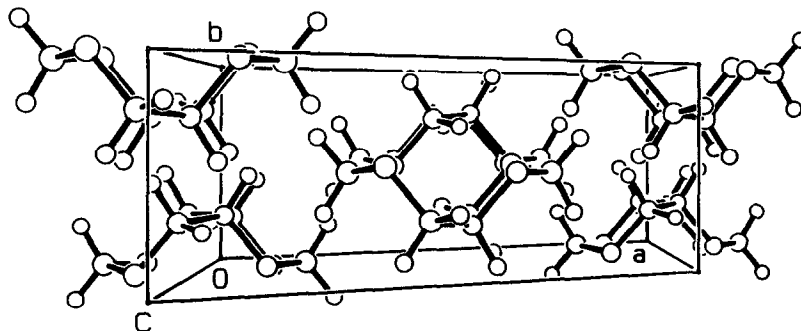
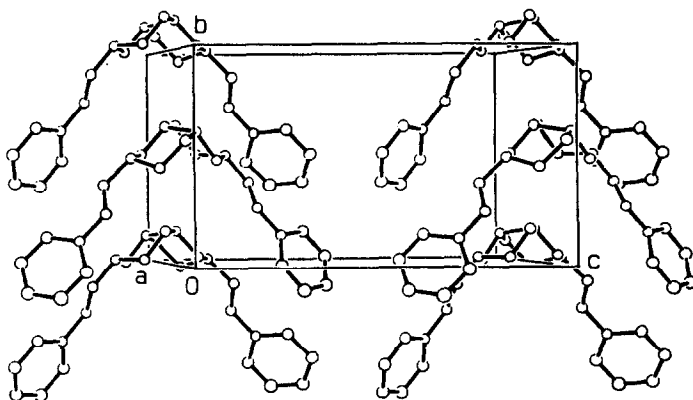


Figure 5. Molecular packing of (9R)-2,6-di-p-(*trans*-styryl)-*cis*-1,3,5,7-tetraoxadecalin (**5**) projected along the a-axis. Hydrogen atoms have been omitted for clarity.



In order to examine the electron density distribution in the molecules, the reflection data was measured carefully at a very low temperature, the complete sphere of data being measured for **2** and a hemisphere for **5**, thereby allowing several measurements of equivalent reflections. For **5** the data were collected to $\sin\theta/\lambda = 1.15$ and the difference electron density maps were generated using the $X-X_{HO}$ method¹⁵, where the high-order atomic coordinates were obtained from a refinement of the data using only those reflections for which $\sin\theta/\lambda$ was greater than 0.7. Unfortunately mechanical restrictions of the diffractometer only allowed the data for **2** to be collected to $\sin\theta/\lambda = 0.8$, so that a satisfactory high-order refinement of the structure was not feasible and the $X-X_{HO}$ maps could not be generated. Therefore standard difference electron density maps were used for the analysis.

Three of a series of difference electron density maps obtained in each of the analyses of **2** and **5** are displayed in Figures 6 and 7, respectively. They represent parallel cross-sections using the plane defined by atoms O1, C2 and O3. The three most significant cross-sections are shown in each of the Figures; contour intervals are at $0.04 \text{ e } \text{Å}^{-3}$, positive electron density is shown in solid lines, negative in short broken lines and the zero level is in longer broken lines. Part (a) shows the cross-section which contains O1, C2 and O3, and, as expected, some weak electron density can be seen lying along the internuclear axes between these atoms. This cross-section should also reveal electron density associated with one of the lone pairs of electrons on each of the atoms O1 and O3. The lone pair lies in the plane of this cross-section and should extend directly out from the ring.

Part (b) shows a cross section parallel to and below (a), being the best plane containing the atoms C4, C10, C9, and C8 (C4, C9', C9 and C4' for compound **2**). Here one can clearly observe that **there is a significant accumulation of electron density along the central C-C bonds**. Part (c) is a cross-section lying above that of (a) at a level which should reveal the electron density associated with the second lone pair of electrons on the atoms O1 and O3. These lone pairs should lie approximately directly above the O1-C9 and O3-C4 bonds respectively. Figure 7 is a "cleaner" map than Figure 6 (which is a property of $X-X_{HO}$ maps), although the crystals of **5** were plate-like, which is not the ideal crystal form for

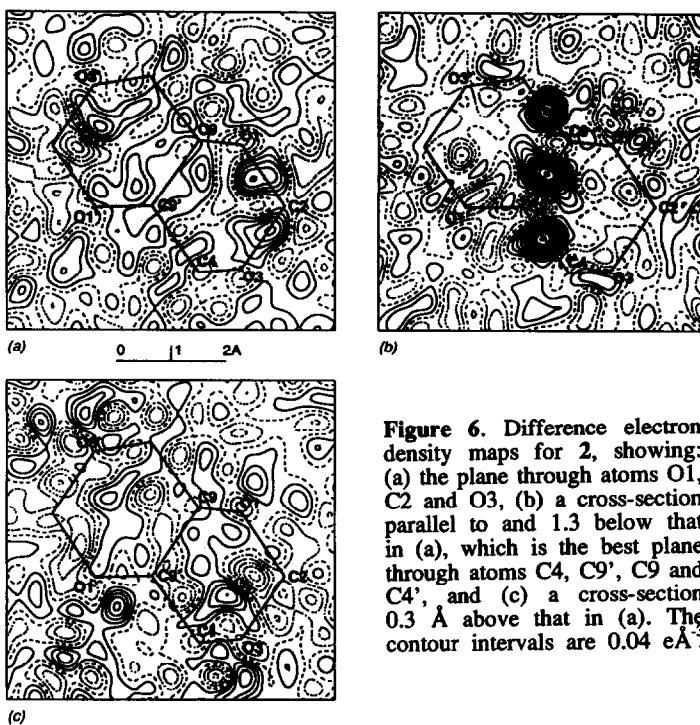


Figure 6. Difference electron density maps for 2, showing: (a) the plane through atoms O1, C2 and O3, (b) a cross-section parallel to and 1.3 Å below that in (a), which is the best plane through atoms C4, C9', C9 and C4', and (c) a cross-section 0.3 Å above that in (a). The contour intervals are 0.04 eÅ⁻³.

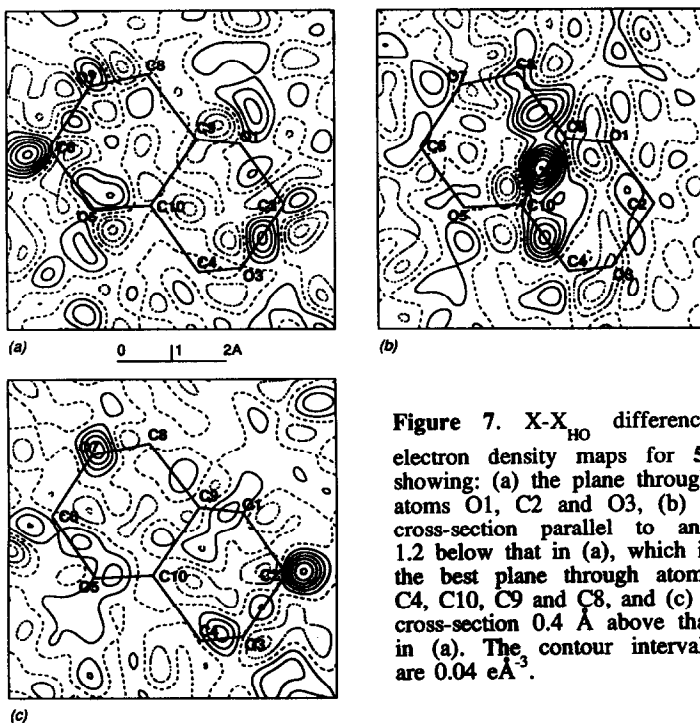


Figure 7. X-X_{HO} difference electron density maps for 5, showing: (a) the plane through atoms O1, C2 and O3, (b) a cross-section parallel to and 1.2 Å below that in (a), which is the best plane through atoms C4, C10, C9 and C8, and (c) a cross-section 0.4 Å above that in (a). The contour intervals are 0.04 eÅ⁻³.

studying accurately the electron density distribution. The search for electron density associated with the lone pairs on the oxygen atoms was somewhat disappointing, although the maps for **5** (Figure 7) look more promising. It appears that the increased electron density in the C-C bonds is the most interesting conclusion of this X-ray diffraction study, in addition to the significant structural information secured.

These observations on the *cis*-1,3,5,7-tetraoxadecalin system should be manifest in its physical properties and the most immediate manifestations are bound to be of structural nature, as will indeed be seen below, including their various consequences. However, there should also be observable spectroscopic manifestations, mainly by NMR, and the ^1H - and ^{13}C -NMR data of **1**^{7a}, **2**^{5,6b,7a} and **5**^{10a} are displayed in Table 4 (3 itself is unavailable and its few existing, as well as new substituted derivatives will be discussed in a separate study).

Table 4. ^1H - and ^{13}C -NMR data of **1**, **2** \rightleftharpoons **3**, and **5** (δ in ppm, J in Hz).

	$\text{H}_{2,6}^{\text{eq}}$	$\text{H}_{2,6}^{\text{ax}}$	$\text{H}_{4,8}^{\text{eq}}$	$\text{H}_{4,8}^{\text{ax}}$	$\text{H}_{9,10}$
1 ^a					
δ	5.01 (d)	4.73 (d)	4.16 (dd)	3.56 (dd)	3.56 (dd)
^1H	$^2\text{J}_{2e,2a}$ -6.2		$^2\text{J}_{4e,4a}$ 8.1	$^3\text{J}_{4a,10}$ 9.3	$^3\text{J}_{4e,10}$ 1.6
^{13}C	94.10		74.06		68.45
2/3					
δ	a) 5.17 (dd) b) 5.12 c) 5.14	4.77 (d)	4.14 (ddd)	3.80 (dd)	3.64 (d)
^1H	$^2\text{J}_{2e,2a}$ -6.1	$^3\text{J}_{2e,4e}$ 0.9	$^2\text{J}_{4e,4a}$ -12.5	$^3\text{J}_{4a,10}$ 1.80 (296 K) 1.83 (313 K) 1.86 (331 K) 1.89 (346 K)	
^{13}C	93.12		69.93		69.39
5 ^a					
δ		5.26 (d)	4.32 (d)	4.05 (d)	3.78 (bs)
^1H		$^2\text{J}_{2a,\text{CH=}}$ 5.1		$^3\text{J}_{4e,4a}$ 12.5	
^{13}C	100.81		69.70		69.70

a) in chloroform-*d*. b) in toluene-*d*₈ at 23 C. c) in toluene-*d*₈ at 73 C.

Our NMR measurements of **2** fit the earlier published⁵ and recently updated ones^{6b,7a}; however, for variable temperature studies we measured it also in toluene-*d*₈, in which the chemical shift order is preserved, although with upshifted values. Strangely, no mention was made in previous literature reports

of the peculiarities in the NMR spectrum of the *cis*-1,3,5,7-tetraoxadecalin system. For one, the methine protons on the C9-C10 bridge of **2** (as well as **5** and its other derivatives¹⁰) resonate at highest field. There seems to be no obvious reason to find them higher than the vicinal, axial methylene protons.

It has been reported, from dipole moment measurements⁵, that *cis*-1,3,5,7-tetraoxadecalin exists in the dynamic equilibrium $2 \rightleftharpoons 3$, in which the O-inside isomer (**2**) is by ca. 90% the preferred one. Since one of our aims was to attain reliable relative stabilities of all the 1,3,5,7-TOD isomers, we examined the dynamic behavior of $2 \rightleftharpoons 3$, using straightforward variable temperature NMR techniques (Nørskov *et al.*^{8b} have investigated a similar equilibrium in a specially prepared disubstituted *cis*-1,3,5,7-TOD system). Spectra of **2** in toluene-*d*₈ were measured in the range 296 - 346 K (Table 4), focussing on ${}^3J_{4,10}^{cis}$ (which is $J_{O-in} = {}^3J_{4a,10}^{cis}$ in **2** and $J_{O-out} = {}^3J_{4e,10}^{cis}$ in **3**), as it changes in the thermally driven equilibrium $2 \rightleftharpoons 3$. While three lower measurements down to 250 K were discarded, since the viscosity of the solution increased appreciably and the slope changed, it should be noted that the lowest ${}^3J_{4,10}$ value reached was 1.5 Hz, which we used for J_{O-in} (in the 2,6-diequatorially substituted, conformationally fixed derivatives of **2** in our hands¹⁰, ${}^3J_{4a,10}$ is in the range of 1.3 - 1.6 Hz). To secure a reliable J_{O-out} value is much more difficult, since **3** itself is not an independently viable species and substituted derivatives (with the desired NMR data) are scarce. Therefore, we had to resort to computational techniques and an MM3 calculation of **3** was carried out and used in conjunction with the PCMODEL molecular modeling program^{16a}, including the option to perform a Karplus type analysis, as modified by Haasnoot *et al.*^{16b}. This gave $J_{O-out} = {}^3J_{4e,10}^{cis} = 6.1$ Hz and ${}^3J_{4a,10}^{trans} = 10.6$ Hz; we could find no literature value for the former, but the latter corroborates well with that (10.61 Hz) observed^{8b} in a substituted derivative of **3**. For comparison, 1,3-dioxane was similarly calculated by MM3/PCMODEL and the relevant NMR coupling constants are (observed values^{17c} in parenthesis): ${}^3J_{4e,5a}^{cis} = 5.1$ (4.9) Hz, ${}^3J_{4a,5e}^{cis} = 2.8$ (2.3) Hz, ${}^3J_{4a,5a}^{trans} = 12.1$ (12.4) Hz and ${}^3J_{4e,5e}^{trans} = 1.2$ (1.2) Hz. The above value for diequatorial ${}^3J_{4e,10}^{cis} = 6.1$ Hz is, indeed, unusually high but, being accompanied by reasonable adjacent values, it reflects the unusual geometry of the ring, as shown below.



Analysing the variable temperature NMR data of *cis*-1,3,5,7-tetraoxadecalin in $2/3$ (Table 4) and using the well known relationships: $J_{obs} = XJ_{O-in} + (1-X)J_{O-out}$ and $\Delta G_T^\circ = -RT \ln K = \Delta H^\circ - T\Delta S^\circ$, one comes up with $\Delta H^\circ = 1.2$ kcal/mol, $\Delta S^\circ = -1$ e.u. and a free energy difference $\Delta G_{296}^\circ = 1.6$ kcal/mol ($K_{296} = 14.4$). Admittedly, due to the mentioned difficulties, mainly in not being able to approach the slow exchange limit, this should be still regarded as approximate and representing lowest values of the thermodynamic parameters for the equilibrium $2 \rightleftharpoons 3$.

The *trans* isomer (**1**) cannot be included in the equilibrium under scrutiny, due to the absence of an accessible isomerization pathway. However, all three isomers can be compared either qualitatively, by interaction-counting^{2a} or computationally (Figure 8). First, and to gain a better understanding, the 1,3,5,7-TOD molecule can be treated as a double 1,3-dioxane system (Figure 8). Stoddart^{7a} and Schroll^{8b} and coworkers have touched upon this point earlier. Thus, one can undertake a fragment analysis of the 1,3,5,7-TOD system in terms of accessible experimental results, since the 1,3-dioxane ring system had been extensively and thoroughly studied¹⁷.

Indeed, considerable insight can be gained by considering the 1,3,5,7-TOD system as constructed of two 4,5-condensed 1,3-dioxane rings, incorporating two intertwined 5-methoxy-1,3-dioxanes and similarly, two 4-methyl-1,3-dioxanes, with their steric and stereoelectronic effects (Figure 8).

Thus (Figure 8a), the relative energies of the 1,3,5,7-TOD isomers were estimated by judiciously combining the experimentally established relative stabilities of: i) axial and equatorial 5-methoxy-1,3-dioxanes^{17,23} (1.5 times the measured value of 1.05 kcal/mol, since the two 1,3-dioxane units overlap in the TOD C9-C10 bond, making one of the four methoxy interactions redundant); ii) similarly, 1.5 times the free energy difference between axial and equatorial 4-methyl-1,3-dioxane^{17c,27a}, as shown in Figure 8. The still unknown relative energy of the *trans*-1,3,5,7-TOD isomer became available this way and, as it turned out, it is the lowest one in the TOD series. However, even taking into account the different experimental methods used for the various fragments, there is only qualitative agreement between the additively estimated (3.5) and the above observed (1.6 kcal/mol) relative energies of *cis*-O-inside (2) vs. *cis*-O-outside (3) isomers.

Figure 8. Relative stabilities of *trans* and the two *cis*-1,3,5,7-tetraoxadecalins, as obtained from interannular fragment analysis and molecular mechanics calculations.

ΔE (exp.)	Relative Energies (kcal/mol) ^a		
	ΔE (calc.)		
(a)	1,3,5,7-tetraoxadecalin (1,3,5,7-TOD)		
	<i>trans</i> (1)	<i>cis</i> -O _i (2)	<i>cis</i> -O _o (3)
5-Methoxy-1,3-dioxane ($\Delta G_{\text{conf.}} = -1.05^{\text{b}}$)	0.0	1.6	0.0
			
4-Methyl-1,3-dioxane ($\Delta G_{\text{conf.}} = -2.95^{\text{c}}$)	0.0	0.0	5.1
			
(b)	0.0	1.6	5.1
MM2-AE ¹⁸	0.6	0.0	5.7
MM3 ¹⁹	1.1	0.0	5.9

a) Entropy differences were neglected.

b) The value is from acid catalysed equilibration studies^{17c,23}, in the least polar solvent.

c) The value is from acid catalysed equilibration studies^{17c,27a}.

d) Steric energies.

A more quantitative evaluation could be expected from molecular mechanics computations and in Figure 8b we included the relative energies of 1, 2 and 3 as calculated by MM2-AE¹⁸ and by MM3^{19,20}. The outcome is intriguing: in *cis*-1,3,5,7-TOD, the steric energy difference between 2 and 3 was calculated to be even higher than the above estimated value, *viz.*, 5.7 and 5.9 kcal/mol, respectively. More surprisingly, the *trans* isomer 1 was calculated to about 1 kcal/mol higher than 2 and not the most stable in the series, *i.e.*, contrary to the results from fragment analysis (Figure 8). These

calculations provided, of course, also the structural parameters of the investigated 1,3,5,7-TOD molecules. Relevant parameters of 1, 2 and 5 are presented in Table 5, to be compared with those taken from the respective X-ray determinations.

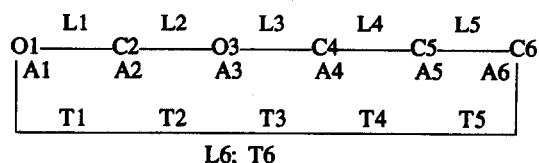
Table 5. Structural parameters of 1, 2 and 5 as obtained from X-ray diffraction analysis and from molecular mechanics (MM2 and MM3) calculations.

	1			2 ^a			5		
	Xray ¹²	MM2	MM3	Xray ^{ab}	MM2	MM3	Xray ^b	MM2	MM3
Bond lengths (Å)									
O(1)-C(2)	1.418	1.416	1.419	1.411	1.413	1.414	1.414	1.416	1.415
O(5)-C(6)		1.416	1.419	1.411	1.413	1.414	1.419	1.416	1.414
O(1)-C(9)	1.430	1.437	1.433	1.436	1.441	1.435	1.438	1.441	1.435
O(5)-C(10)		1.437	1.433	1.436	1.441	1.435	1.437	1.440	1.434
O(3)-C(2)	1.416	1.416	1.419	1.413	1.413	1.414	1.421	1.416	1.414
O(7)-C(6)		1.416	1.419	1.413	1.413	1.414	1.416	1.416	1.414
O(3)-C(4)	1.439	1.441	1.435	1.434	1.438	1.432	1.435	1.438	1.431
O(7)-C(8)		1.441	1.435	1.434	1.438	1.432	1.442	1.438	1.432
C(4)-C(10)		1.519	1.524	1.510	1.523	1.530	1.519	1.521	1.528
C(8)-C(9)		1.519	1.524	1.510	1.523	1.530	1.514	1.521	1.528
C(9)-C(10)		1.519	1.527	1.529	1.523	1.534	1.528	1.520	1.531
Bond angles (degrees)									
C(2)-O(1)-C(9)	109.0	109.7	108.8	110.8	110.9	110.5	111.4	111.9	111.5
C(6)-O(5)-C(10)		109.7	108.8	110.8	110.9	110.5	111.4	112.2	111.7
C(2)-O(3)-C(4)	111.0	111.1	110.6	109.8	110.5	110.2	110.6	111.4	111.1
C(6)-O(7)-C(8)		111.1	110.6	109.8	110.5	110.2	110.5	111.4	111.0
O(1)-C(2)-O(3)	112.4	111.1	112.6	112.1	110.1	111.5	111.3	106.7	106.9
O(5)-C(6)-O(7)		111.1	112.6	112.1	110.1	111.5	111.1	106.8	107.1
O(3)-C(4)-C(10)		107.9	107.2	111.3	109.9	109.9	111.5	109.6	109.5
O(7)-C(8)-C(9)		107.9	107.2	111.3	109.9	109.9	111.1	109.7	109.7
O(1)-C(9)-C(8)		111.9	110.5	108.6	109.1	108.1	108.1	109.0	108.1
O(5)-C(10)-C(4)		111.9	110.5	108.6	109.1	108.1	107.7	108.9	107.8
O(1)-C(9)-C(10)		108.3	106.6	110.2	109.7	109.1	110.3	109.6	108.9
O(5)-C(10)-C(9)		108.3	106.6	110.2	109.7	109.1	110.8	109.4	108.7
C(4)-C(10)-C(9)		108.6	109.4	110.1	110.5	111.9	110.7	110.0	111.5
C(8)-C(9)-C(10)		108.6	109.4	110.1	110.5	111.9	110.5	109.9	111.4
Torsion angles (degrees)									
C(2)-O(1)-C(9)-C(8)		179.5	179.6	176.4	178.3	178.2	176.6	179.1	179.4
C(6)-O(5)-C(10)-C(4)		179.5	179.6	176.4	178.3	178.2	176.2	179.1	179.6
C(2)-O(1)-C(9)-C(10)		-60.8	-61.6	55.8	57.1	56.2	55.7	58.7	58.3
C(6)-O(5)-C(10)-C(9)		-60.8	-61.6	55.8	57.1	56.2	55.0	58.8	58.5
C(9)-O(1)-C(2)-O(3)	61.7	63.1	64.1	-63.3	-65.1	-65.9	-63.4	-66.4	-68.7
C(10)-O(5)-C(6)-O(7)		63.1	64.1	-63.3	-65.1	-65.9	-62.9	-66.2	-68.6
C(2)-O(3)-C(4)-C(10)		58.8	57.4	-56.5	-57.7	-55.6	-55.5	-59.7	-58.4
C(6)-O(7)-C(8)-C(9)		58.8	57.4	-56.5	-57.7	-55.6	-56.6	-59.6	-58.1
C(4)-O(3)-C(2)-O(1)	-62.3	-62.6	-62.2	63.0	65.3	65.3	62.7	66.7	68.4
C(8)-O(7)-C(6)-O(5)		-62.6	-62.2	63.0	65.3	65.3	63.3	66.3	67.8
O(3)-C(4)-C(10)-O(5)		-176.2	-175.1	-69.8	-70.2	-71.4	-72.4	-70.2	-71.8
O(7)-C(8)-C(9)-O(1)		-176.2	-175.1	-69.8	-70.2	-71.4	-71.4	-70.1	-71.9
O(3)-C(4)-C(10)-C(9)		-56.7	-58.0	50.8	50.5	48.8	48.9	49.8	47.5
O(7)-C(8)-C(9)-C(10)		-56.7	-58.0	50.8	50.5	48.8	49.4	50.0	47.7
O(1)-C(9)-C(10)-O(5)		180.0	180.0	69.6	70.4	70.8	71.0	70.4	71.6
O(1)-C(9)-C(10)-C(4)		58.3	60.5	-50.0	-50.0	-48.9	-48.4	-49.1	-47.2
O(5)-C(10)-C(9)-C(8)		58.3	60.5	-50.0	-50.0	-48.9	-48.5	-49.4	-47.5
C(8)-C(9)-C(10)-C(4)		180.0	180.0	-169.7	-170.4	-168.6	-167.9	-168.9	-166.2

a. A crystallographic C2 axis through C(9)-C(10) makes atoms O5, O7, C6, C8 & C10 equivalent to O1, O3, C2, C4 & C9, respectively. b. X-ray data are given without standard deviations and rounded off for comparison with calculated data. The complete list is included in the Supplementary Material.

It appears that bond angles and torsion angles are rather well reproduced by calculation; as to bond lengths, however, only those in the C-O-C-O-C anomeric moiety were faithfully reproduced but not so the C-C bonds, for which the calculations could not match the unusually short observed ones. This inability of MM2 and MM3 to calculate faithfully relative stabilities and geometries in the TOD series is puzzling and may be due to some failure in the MM force fields to account correctly for the stereoelectronic effects operating in the TOD molecules. It is certainly impedimental to further detailed study of these systems. Therefore, it will have to be urgently dealt with⁹.

Table 6. Mean bond lengths (L, Å), bond angles (A, deg.) and dihedral angles (T, deg., absolute values) of 1,3-dioxane systems retrieved from the CSD with m.s.d.'s in parentheses.



Cases:	All	Monocyclic substit.	Monocyclic 5-axially substituted	Monocyclic 5-equatorially substituted	Within 1,3,5,7-TOD
Hits:	109	23	11	10	5
	Mean Value (m.s.d.)				
L1	1.415 (0.002)	1.410 (0.004)	1.414 (0.004)	1.410 (0.004)	1.413 (0.003)
L2	1.410 (0.002)	1.402 (0.005)	1.406 (0.007)	1.403 (0.005)	1.411 (0.003)
L3	1.432 (0.001)	1.432 (0.003)	1.432 (0.004)	1.436 (0.003)	1.434 (0.004)
L4	1.519 (0.002)	1.521 (0.004)	1.522 (0.004)	1.530 (0.006)	1.520 (0.005)
L5	1.517 (0.002)	1.508 (0.004)	1.515 (0.005)	1.522 (0.005)	1.513 (0.005)
L6	1.432 (0.001)	1.432 (0.003)	1.431 (0.004)	1.434 (0.003)	1.430 (0.003)
A1	111.58 (0.18)	111.46 (0.32)	111.77 (0.51)	110.51 (0.34)	110.48 (0.69)
A2	110.83 (0.11)	111.06 (0.23)	110.49 (0.24)	110.94 (0.37)	112.21 (0.29)
A3	112.02 (0.18)	111.79 (0.37)	111.90 (0.47)	110.85 (0.54)	111.50 (0.59)
A4	109.95 (0.17)	110.13 (0.26)	110.43 (0.50)	110.02 (0.35)	108.20 (1.05)
A5	108.73 (0.21)	108.49 (0.42)	107.91 (0.67)	106.86 (0.42)	109.89 (0.69)
A6	109.98 (0.18)	110.21 (0.34)	111.08 (0.39)	110.44 (0.40)	109.90 (0.38)
T1	60.54 (0.44)	59.65 (1.43)	58.97 (2.34)	62.45 (0.50)	61.85 (1.41)
T2	60.49 (0.41)	60.07 (1.19)	58.25 (2.86)	62.58 (0.66)	63.26 (0.75)
T3	57.20 (0.34)	57.49 (0.57)	58.76 (1.81)	59.16 (0.93)	58.12 (1.07)
T4	52.48 (0.60)	51.06 (1.90)	51.29 (1.23)	54.33 (1.01)	53.34 (2.02)
T5	53.19 (0.45)	52.76 (0.60)	48.50 (3.76)	54.63 (0.51)	53.67 (2.64)
T6	57.79 (0.33)	58.20 (0.89)	57.90 (0.85)	59.33 (0.51)	57.08 (1.88)

Still in this context, we were interested in the details of the ring geometry of as large a number as possible of 1,3-dioxane derivatives, so that they could be statistically analysed and compared with those in available 1,3,5,7-TOD structures (*cf.* Table 5 and ref. 11). This was accomplished by retrieving 1,3-dioxane systems from the Cambridge Structural Database (CSD)²⁶ and submitting them to careful screening and purging of spurious items, in order to maximize accuracy and consistency. This qualifying procedure left 109 items for statistical analysis (Table 6).

The structural parameters characteristic of 1,3-dioxanes and relevant to this work, (see also earlier discussions^{17,27,28}), can be soundly generalized as follows (Table 6): (i) there is increased ring puckering of the acetal part (C-O-C-O dihedral angles T1 and T2, around 60°), as compared with that of the carbocyclic part (O-C-C-C dihedral angles T4 and T5 around 53°); (ii) the O-C-O bond lengths are short (L1 and L2 around 1.41 Å) and the C-O-C-O-C bond angles, A1, A2 and A3 are large (110-112°) as imposed by the *anomeric effect*^{13,14}; (iii) there is a characteristic C-C bond shortening (L4 and L5 around 1.52 Å), as actually demanded of electronegatively substituted C-C bonds²⁹.

This can be now instructively compared with the 1,3,5,7-TOD data obtained in this study (Table 5) along with some which have been retrieved from the literature¹¹ (Table 6, last column). It is evident that some of the 1,3,5,7-TOD parameters are similar to those in the 1,3-dioxane rings, such as the ones associated with the O-C-O (*anomeric effect*) moiety, *i.e.*, short bond lengths (1.41 Å) but there is higher relative ring-puckering in this part of the TOD rings (C-O-C-O dihedral angles of 63°). At the same time the C-C-C bonds in the TOD molecules are even shorter (*ca.* 1.51 Å) and are accompanied by considerable more flattening of that part of the ring, *i.e.*, O-C-C-C dihedral angles of 50° and below (Table 5, bottom). This compares well with the 5-axially substituted 1,3-dioxanes (Table 6, third column).

All the above described findings contribute to the understanding of the overall structural picture of the 1,3,5,7-TOD diastereomers, in particular *cis*-1,3,5,7-TOD including its above discussed peculiar NMR chemical shifts and vicinal coupling constants. The latter, in particular $J_{\text{O-out}}$ (*vide supra*) are a result of the increased ring flattening in the C-C-C part of the 1,3-dioxane rings, whereas the unusually high field chemical shift of the angular protons is brought about by the high electron density in these bonds, which correlates (inversely) well with the considerable bond shortening in the C-C-C-C moiety, as postulated previously³⁰. As to why the C-C bond shortening and the *trans* relative stability are not well calculated by the MM force fields, it stands to reason that it is because both MM2¹⁸ and MM3¹⁹ have not been parametrized for such, rather esoteric features, essentially of stereoelectronic nature; this will have to be, of course, substantiated⁹.

Finally, we want to mention also the interesting packing arrangements of the *cis*-TOD's, namely, the racemic **2** (Figure 4) crystallised accordingly (C2/c space group) whereas the optically active **5** (Figure 5) crystallized in the chiral P2₁ space group, adopting a typical host-guest arrangement.

CONCLUSIONS

A low temperature X-ray diffraction study of *cis*-1,3,5,7-tetraoxadecalin (**2**) and its 2,6-di(*trans*-styryl) derivative (**5**) provided their detailed structures and electron density properties, including a peculiar density concentration in the central C-C bonds. In solution, the dynamic behavior

of 2 was probed using variable temperature NMR techniques. The *cis*-O-inside/O-outside (2 \rightleftharpoons 3) equilibrium occurs in toluene with a free energy difference ΔG°_{298} of more than 1.6 kcal/mol. The relative energies from the solution studies and the structural parameters from the X-ray analysis were compared with the results from fragment analysis, based on available structural and relative stability data of appropriately substituted 1,3-dioxanes and other small units. This approach indicated that the *trans* (1) isomer is the most stable one in the TOD manifold and evaluated ΔG° for 2 \rightleftharpoons 3 at 3.5 kcal/mol. Analysis of structural data of 1,3-dioxanes and 1,3,5,7-tetraoxadecalins retrieved from the Cambridge Structural Database provided a consistent understanding of the TOD structural features. Molecular mechanics calculations using MM2 and MM3, however, performed poorly in reproducing experimental energies and certain structural parameters. The treatment of this problem was deferred to the following paper.

Acknowledgments. This work was supported in part by a research grant from the Ministry of Science and Arts and a grant from the Ministry of Absorption (to L. G.). The molecular mechanics calculations at Tel-Aviv were performed on a DEC 5000/200 workstation which was purchased with partial support from the Sackler Fund.

REFERENCES

1. Structure and Conformation of Heterocycles. 25. Part 24: Senderowitz, H., Aped, P., Fuchs, B. *Tetrahedron* **1993** *49*, 3879.
2. a. Eliel, E.L., Allinger, N.L., Angyal, S.J., Morrison, G.A. "Conformational Analysis", Interscience, New York, 1965: p. 231
b. Anet, F. A. L., Anet, R. in "Dynamic NMR Spectroscopy" L. M. Jackman F. A. Cotton (Eds.), Ch. 14, Academic Press New York 1975.
3. a. Goldberg, I., Shmueli, U., Fuchs, B. *J. Chem. Soc., Perkin II*, **1972**, 357.
b. Aped, P., Fuchs, B., Goldberg, I., Senderowitz, H., Schleifer, L., Tartakovsky, E., Anteonis, M., Borremans, F. *Tetrahedron* **1991**, *47*, 5781.
c. Senderowitz, H., Golender, L., Fuchs, B., submitted for publication.
4. a. Barker, S. A., Bourne, E. J. *Adv. Carbohydr. Chem.* **1952**, *7*, 138.
b. Mills, A. *Adv. Carbohydr. Chem.* **1955**, *10*, 1.
c. Stoddart, J. F. "Stereochemistry of Carbohydrates", p. 210, Wiley, New York, 1971.
d. Foster, A. B. in "The Carbohydrates", W. Pigman and D. Horton, Eds., Vol. 1A, Ch. 11, Academic Press, New York, 1972.
5. Lemieux, R. U., Howard, J. *Can. J. Chem.*, **1963**, *41*, 393.
6. a. Nougquier, R., Gras, J.-L., Mchich, M. *Tetrahedron*, **1988**, *44*, 2943.
b. Gras, J.-L., Poncet, A. *Synth. Commun.* **1992**, *22*, 405.
7. Burden, I. J., Stoddart, J. F. *J. Chem. Soc., Perkin I* **1975**, a. 666; b. 675.
8. a. Jensen, R. B., Buchardt, O., Jørgensen, S. E., Nielsen, J. U. R., Schroll, G., Altona, C. *Acta Chem. Scand. B* **1975** *29B*, 373.
b. Nørsköv, L., Jensen, R. B., Schroll, G. *Acta Chem. Scand. B* **1983** *37B*, 133 and previous parts in

this series.

9. For a detailed discussion of stereoelectronics in the TOD system see following article.
10. a. Abramson, S., Ashkenazi, E., Goldberg, I., Greenwald, M., Jatzke, H., Vardi, M., Weinman, S., Fuchs, B., *J. Chem. Soc. Chem. Commun.*, in press.
b. Frische, K., Greenwald, M., Abramson, S., Fuchs, B., *J. Chem. Soc. Chem. Commun.*, in press.
11. a. Kohne, B., Praefcke, K., Omar, R. S., Frolow F. *Z. Naturforsch.* **1986**, *B41*, 736.
b. Glebova, Z. I., Polenov, V. A., Uzlova, L. A., Zhdanov, Yu. A., Yanovskii, A. I., Struchkov, Yu. T. *Zh. Obshch. Khim.* **1987** *57*, 104.
c. Bernstein, J., Green, B. S., Rejto M. *J. Am. Chem. Soc.* **1980** *102*, 323.
d. Smith, D. A., Baker, D., Rahman A. F. M. M. *Struct. Chem.* **1991** *2*, 65.
e. Grindley, T. B., Kusuma, S., Cameron, T. S., Kumari A. *Carbohydr. Res.* **1987** *159*, 171.
f. Koll, P., John, H.-G., Kopf J. *Liebigs Ann. Chem.* **1982**, 639.
12. Nørskov-Lauritsen, L., Allinger, N. L. *J. Comput. Chem.* **1984** *5*, 326.
13. a. Szarek, W.A., Horton, Editors, "Anomeric Effect. Origins and Consequences", A.C.Symposia Series, Vol.87, Washington, D.C. **1979**.
b. Kirby, A.J., "The Anomeric Effect and Related Stereoelectronic Effects at Oxygen" Springer Verlag, Berlin, **1983**.
c. Deslongchamps, P., "Stereoelectronic Effects in Organic Chemistry", Wiley, New York **1983**.
14. a. Aped, P., Apeloig, Y., Ellencweig, A., Fuchs, B., Goldberg, I., Karni, M., Tartakovsky E *J. Am. Chem. Soc.* **1987** *109*, 1486.
b. Schleifer, L., Senderowitz, H., Aped, P., Tartakovsky, E., Fuchs, B. *Carbohydrate Res.* **1990** *206*, 21.
c. Fuchs, B., Schleifer, L., Tartakovsky, E., *Nouv. J. Chim.* **1984** *8*, 275.
15. Cameron, T. S., Borecka, B. *Phosphorus, Sulfur, and Silicon* **1992**, *64*, 121.
16. a. PCMODEL, Available from Serena Software, Box 3076, Bloomington, IN 47402, USA.
b. Haasnoot, C. A. G., DeLeeuw, L., Altona, C. *Tetrahedron* **1981** *36*, 2783.
17. a. Eliel, E. L. *Angew. Chem., Int. Ed. Engl.* **1972** *11*, 739.
b. Eliel, E. L. *Pure Appl. Chem.* **1971** *25*, 509.
c. Anteunis, M. J. O., Tavernier, D., Borremans, F. *Heterocycles* **1976** *4*, 293.
c. Riddell F. G. *The Conformational Analysis of Heterocyclic Compounds* Ch. 4 & 5, Academic Press, London 1980.
18. a. Our modification of MM2-87 for the anomeric effect in O-C-O systems, MM2-AE^{14a} was used:
b. Allinger, N. L., Yuh, Y. H., Profeta, S., *QCPE Program 406*, University of Indiana, Bloomington, IN 47401.¹²
c. Allinger, N. L. *J. Am. Chem. Soc.* **1977** *99*, 8127.
d. Allinger, N. L., Chang, S. H. M., Glaser, D. H., Honig, H. *Isr. J. Chem* **1980** *20*, 5.
e. Profeta, S., Allinger, N. L. *J. Am. Chem. Soc.* **1985** *107*, 1907, and references therein.
19. a. MM3 is available from Technical Utilization Corporation, Inc., 235 Glen Village Court, Powell, Ohio 43065 and Tripos Associates, 1699 S. Hanley Road, St. Louis, Missouri 63144.
b. Allinger, N. L., Yuh, Y. H., Lii, J.-H. *J. Am. Chem. Soc.* **1989** *111*, 8551 and subsequent articles, in particular that on alcohols and ethers.²⁰

20. Allinger, N. L., Rahman, M., Lii, J.-H. *J. Am. Chem. Soc.* **1990** *112*, 8293.
21. Sheldrick, G. M.: SHELXS-86, in "Crystallographic Computing 3", Eds. G. M. Sheldrick, C. Kruger and R. Goddard, Oxford University Press, 1985, pp. 175-189.
22. TEXSAN-TEXRAY Single Crystal Structure Analysis Package, Version 5.0. Molecular Structure Corporation, The Woodlands, Texas (1989).
23. a. Eliel, E. L., Hofer, O. *J. Am. Chem. Soc.* **1973**, *95*, 8041
b. Abraham, R. J., Banks, H. D., Eliel, E. L., Hofer, O., Kaloustian, M. K. *J. Am. Chem. Soc.* **1972**, *94*, 1913.
24. a. Oyanagi, T., Kuchitsu, K. *Bull. Chem. Soc. Japan* **1978** *51*, 2237.
b. Hayashi, M., Kuwada, K. *J. Mol. Struct.* **1975** *28*, 147.
25. Heenan, R. K., Bartell, L. S. *J. Chem. Phys.* **1983** *78*, 1270 and previous work cited there.
26. Allen, F. H., Bellard, S., Brice, M. D., Cartwright, B. A., Doubleday, A., Higgs, H., Hummelink, T., Hummelink-Peters, B. G., Kennard, O., Motherwell, W. D. S., Rodgers, J. R., Watson D. G. *Acta Cryst.* **1979** *35*, 2331.
27. a. Eliel, E. L., Knoeber, Sr. M. C. *J. Am. Chem. Soc.* **1968**, *90*, 3444.
b. Nader, F. W., Eliel, E. L. *J. Am. Chem. Soc.* **1970**, *92*, 3050.
28. de Kok, A. J., Romers, C. *Rec. Trav. Chim.* **1970** *89*, 313.
29. Allinger, N. L., Imam, M. R., Frierson, M. R., Yuh, Y., Schäfer, L., *Mathematics and Computational Concepts in Chemistry*, N. Trinajstić, Ed., E. Horwood, London, **1986** p. 8.
30. Berkovich-Yellin, Z., Leiserowitz, L. *J. Am. Chem. Soc.* **1975**, *97*, 5627.

(Received in UK 4 March 1994; revised 15 June 1994; accepted 24 June 1994)